Pep-Lipid Cubosomes and Vesicles Compartmentalized by Micelles from Self-Assembly of Multiple Neuroprotective Building Blocks Including a Large Peptide Hormone PACAP-DHA

Angelina Angelova, Markus Drechsler, Vasil M Garamus, Borislav Angelov

Pep-Lipid Cubosomes and Vesicles Compartmentalized by Micelles from Self-Assembly of Multiple Neuroprotective Building Blocks Including a Large Peptide Hormone PACAP-DHA

Angelina Angelova,*[1] Markus Drechsler[2], Vasil M. Garamus[3], Borislav Angelov[4]

Abstract: Structural control over design and formation of self-assembled nanomaterials for neuroprotection and neuroregeneration is crucial for their application in nanomedicine. Here a synthetic construct of the pituitary adenylate cyclase-activating polypeptide (PACAP38) coupled to a docosahexaenoic acid (DHA: an ω-3 polyunsaturated fatty acid (PUFA)) is designed towards the creation of compartmentalized liquid crystalline assemblies of neuroprotective compounds. The hormone PACAP38 is a ligand of the class B PAC1 G-protein-coupled receptor (GPCR), whereas DHA is a lipid trophic factor. The lipidated peptide PACAP-DHA is co-assembled into hierarchical nanostructures elaborated from hybrid vesicle-micelle reservoirs as well into PEGylated cubosomes composed of multiple neuroprotective building blocks. The resulting nanostructures are determined by synchrotron small-angle X-ray scattering (BioSAXS) and cryogenic transmission electron microscopy (cryo-TEM). Multicompartment topologies are obtained in a two-fold approach: (i) intriguing compartmentalized vesicles, which embed pep-lipid micelles forming nanopatterns, and (ii) multidomain pep-lipid cubosomes. Both kinds of topologies are favorable for sustained-release applications in combination therapies of neurodegeneration. The organizational complexity of the scaffolds involving the lipidated high-molecular weight peptide hormone is beyond the one that has been reached with small lipid-like peptide surfactants.

Introduction

Current concepts in design of synthetic biomimetic assemblies are highly productive for the fields of internally nanostructured materials, nanoparticles of mesoporous topologies, nanosheets, nanotubules, biocompatible scaffolds and hierarchical type constructs as well as for understanding of living nanoscale topologies and biomembranes dynamics.[1-7] The progress in nanomedicine and regenerative therapies is increasingly focused on smart nanocarriers for drug delivery and supramolecular nanoprodrugs of improved efficacy.[6-9] Self-assembly of prodrugs into nanoparticles can ensure high drug content and carrier-free drug delivery.[8,9] The attachment of lipophilic moieties to hydrophilic drug molecules enhances the bioavailability of the therapeutic agents.[8] Despite that various peptides have been modified by anchoring of hydrophobic acyl chains (lipidated peptides), the resulting structures have scarcely been composed of neuroprotective molecules.[3c,10] At variance, extensive research has been reported on self-assembly of antimicrobial and anticancer peptides and the destabilization of lipid membranes.[1a,3a,3b,9b,11,12]

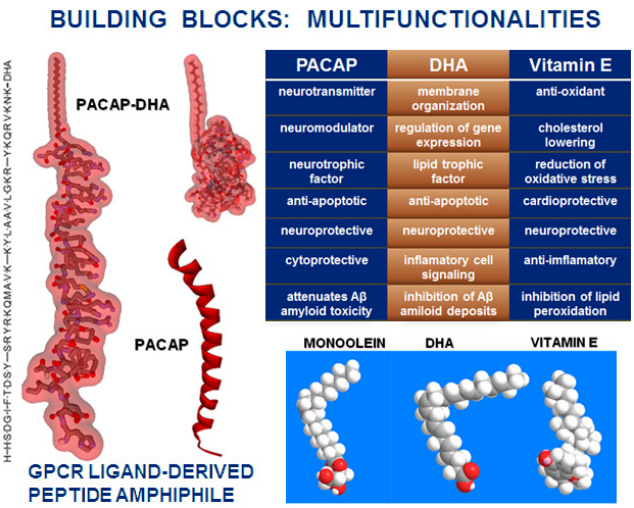

Figure 1. Strategy for co-assembly of multiple molecular building blocks with neuroprotective functionalities involving a GPCR ligand-derived peptide amphiphile PACAP-DHA. The synthetic construct comprises the pituitary adenylate cyclase-activating polypeptide (PACAP38) and the long-chain ω-3 polyunsaturated fatty acid DHA (C22:6). The lipidated peptide hormone is presented in an extended state (left) and in a folded configuration (right) with regard to the non-modified PACAP38 peptide (bottom panel). The key biological functions of the building blocks PACAP, DHA (docosahexaenoic acid), and vitamin E (α-tocopherol) are schematically indicated (see details and references in SI for the choice of the molecules).

Neurodegenerative diseases (Alzheimer's (AD) and Parkinson's diseases, and amyotrophic lateral sclerosis (ALS)) are multi-factor disorders and therefore require targeting of multiple signaling pathways towards regeneration.[13] The necessity of alternative concepts and delivery approaches has been emphasized by the fact that symptom-modifying medicines have failed to treat the inherent causes of neurodegeneration.[13]

[1] Corresponding Author: Dr.(H.D.R.) A. Angelova
Institut Galien Paris-Sud, CNRS UMR 8612, Univ. Paris-Sud, Université Paris-Saclay, LabEx LERMIT, F-92290 Châtenay-Malabry, France
E-mail: Angelina.Angelova@u-psud.fr
[2] Dr. M. Drechsler
Keylab "Electron and Optical Microscopy", Bavarian Polymerinstitute (BPI), University of Bayreuth, D-95440 Bayreuth, Germany
[3] Dr. V.M. Garamus,
Helmholtz-Zentrum Geesthacht: Centre for Materials and Coastal Research, D-21502 Geesthacht, Germany
[4] Dr. B. Angelov
Institute of Physics, ELI Beamlines, Academy of Sciences of the Czech Republic, Na Slovance 2, CZ-18221 Prague, Czech Republic

Supporting information for this article is given *via* a link at the end of the document.

We consider multifunctional self-assembled cubosome nanoparticles (with internal compartments for enhanced upload of neuroprotective molecules) as excellent candidates for innovation in neuro-regenerative therapies.[1c,7b,13b] In this perspective, we investigate the co-assembly of several therapeutic building blocks into interface-rich hierarchically-organized biocompatible nanostructures. Figure 1 presents the compounds used here as building blocks. Among the considered lipophilic moieties, docosahexaenoic acid (DHA) (C22:6) is chosen as a natural long chain PUFA, which is especially beneficial for human health.[14] The bioactive building block DHA plays a crucial role in the control of the phospholipid membrane organization.[14b] Our recent super-resolution STED nanoscopy investigation has revealed the DHA effect on the nanoscale clustering and oligomerization of the neurotrophin receptor TrkB, which is responsible for the neuronal cell survival and function.[14c]

In the present design, the lipid trophic factor DHA is bound to the neuropeptide PACAP [a second therapeutic building block of 38 amino acids] in order to create a new bioactive amphiphile PACAP-DHA (Fig. 1). PACAP is a high-molecular-weight neuropeptide ligand of the PAC1 membrane receptor (a class B GPCR).[15,16a] The peptide exhibits strong anti-apoptotic effects in neuronal and non-neuronal cells and appears to be a neurotrophic factor.[15,16] Both PACAP and DHA are deficient under pathological and stress conditions and must be delivered by nanocarriers. High resolution structural methods, such as synchrotron BioSAXS and cryo-TEM imaging, are indispensable for deeper understanding how to achieve pep-lipid scaffolds as reservoirs with sustained-release properties.

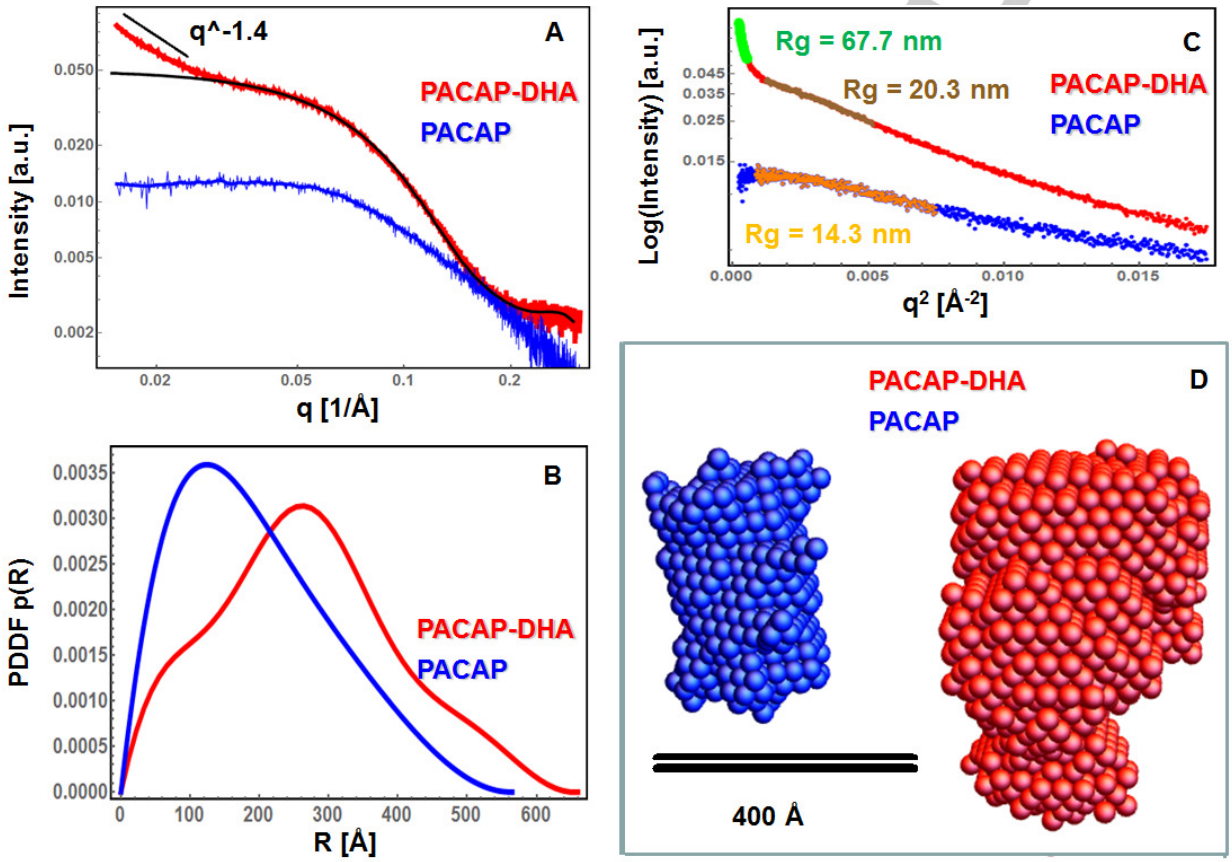

Figure 2. (A) Synchrotron small-angle X-ray scattering (SAXS) patterns of the lipidated peptide hormone PACAP-DHA (PACAP bound to a docosahexaenoic acid DHA) at concentration 29 mg/mL (equal to 6 mM) (red plot) and of the native PACAP polypeptide (blue plot; 10 mg/mL concentration) in solution phase at 20 °C. The fitted plot without large aggregates (black curve overlay) visibly deviates from the aggregation slope (black line). (B) Pair Distance Distribution Functions (PDDF) corresponding to PACAP (blue plot) and PACAP-DHA (red) solutions. (C) Guinier plot for determination of the Rg in case of the aggregated PACAP-DHA (green overlay) and non-aggregated PACAP-DHA (brown overlay) and PACAP (orange overlay). (D) Representative 3D dummy atom models derived from the PDDF (panel B) for PACAP (blue) and PACAP-DHA (red).

Our structural approach includes BioSAXS investigations of the nanostructures resulting from the self-assembly of the amphiphile of major interest PACAP-DHA alone and in mixtures with additional safe compounds (Fig. 1) that may yield hybrid assemblies with compartmentalized organization involving bilayer building blocks. To ensure the steric stability of the dispersed nanoparticles, we included in the assemblies the PEGylated amphiphile vitamin E α-tocopheryl polyethylene glycol 1000 succinate (VPGS-PEG_{1000}), which has been known as a safe surfactant.[17a] Preliminary BioSAXS experiments have established that PACAP-DHA has no strong affinity for assembly with VPGS-PEG_{1000} micelles used as a single-component

biomimetic membrane medium. Therefore, two new types of multicomponent amphiphilic mixtures were studied by SAXS and cryo-TEM towards nanostructure determinations: (i) PACAP-DHA/vitamin E/VPGS-PEG$_{1000}$ and (ii) PACAP-DHA/MO/DHA/vitamin E/VPGS-PEG$_{1000}$. The choice of the nonlamellar lipid monoolein (MO),[17-19] forming multicompartment vehicles such as cubosomes, and the molar ratios between the components was done based on preliminary structural experiments and the existing knowledge from our previous publications on phase behaviour of nanostructured lyotropic liquid crystalline lipid mixtures serving for biomolecular encapsulation.[1c,6a,17,18a,18b,20] Here, we present the amphiphilic compositions for which the obtained structural data suggest potential interest for application of PACAP-DHA-embedding assemblies in future neuronanomedicine research.

Results and Discussion

Scattering patterns of PACAP-DHA and PACAP peptides in solutions

We compared the SAXS patterns of PACAP-DHA and PACAP peptides in solutions. The PACAP-DHA peptide amphiphile was custom synthesized by coupling the polyunsaturated DHA to the free Lys-38 residue of the C-terminal of the PACAP38 polypeptide. Figure 2A shows the SAXS pattern of the lipidated PACAP-DHA with regard to that of the native polypeptide PACAP (presented in Fig. 1). PACAP-DHA shows a visible aggregation with a slope ~$q^{-1.4}$. Such aggregates could be interpreted as an early stage of formation of loosely textured mass fractals and a presence of elongated objects that are not able to produce rough or smooth surfaces (~q^{-4}).

The difference in the recorded solution scattering curves reveals a structural change in the supramolecular organization of the polypeptide owing to the covalent coupling of the long chain ω-3 PUFA. The distance distribution p(r) function derived from the SAXS pattern (Fig. 2B), excluding the low *q* region with aggregation, evidenced that the peptide amphiphile PACAP-DHA self-assembles into nanoparticles with a maximum diameter ~65 nm (Fig.2B red curve). The shape of *p(r)* has a left and right bumps and a tail on the right side. The bump on the left hints for the existence of smaller objects with a radius in the range 6-7 nm possibly analogous to a single PACAP-DHA micelle. In the case of PACAP, the *p(r)* (blue curve) is typical for cylindrical objects. The maximum distance was determined to be ~55 nm.

For the investigated PACAP-DHA concentration (6 mM equal to 29 mg/ml), the estimated gyration radius, Rg, of 67.7 nm from the Guinier plot (Fig. 2C) corresponds to a notable macromolecular clustering or aggregation (~$q^{-1.4}$) in the aqueous medium. The slope of the scattering curve (without the low *q*-values) and its overall shape gave a possibility for determination of a smaller Rg = 20.3 nm that can be assigned to the nanoparticles building the larger aggregate. A coexistence of prolate and spherical nanoparticles in the dispersion cannot be excluded for such a system (see ref. 12d for the BioSAXS modeling approach). The propensity of the concentrated peptide for clustering and aggregation may be explained by the hydrophobic interactions between the lipid moieties of the PACAP-DHA macromolecules and/or by the association of the hydrophobic N-terminal regions of the polypeptide chains. Until now, the unmodified PACAP polypeptide has only been solubilized in dodecylphosphocholine phospholipid micelles for a NMR study.[16a]

An experimental gyration radius value, Rg, of 14.3 nm was determined by Guinier plot for the native peptide PACAP38 in a concentrated solution (10 mg/mL) state (Figure 2C). A gyration radius value Rg of 2.2 nm was obtained for PACAP in a monomeric state upon 10 fold dilution.

Figure 2D shows the 3D dummy atom reconstruction based on the PDDF *p(r)* function from panel 2B using the DAMMIN program from ATSAS package for BioSAXS analysis.[25] Twenty different reconstructions of both systems were averaged with the DAMAVER program from the same software package to get more representative models. In the case of native PACAP, the overall shape resembles a prolate or a barrel like nanoparticle with a length ~35 nm and a radius ~15 nm close to the obtained Rg (Fig. 2C). The PACAP-DHA reconstruction gave a larger object with a length reaching ~50 nm and a pear-like shape. Because of the aggregation, the PACAP-DHA system cannot be considered as a monodisperse and the pear shape could be a result of the coexistence of prolate and spherical objects in the mixture.

Co-assembly of PACAP-DHA with a neuroprotective amphiphile in a PEGylated surfactant environment

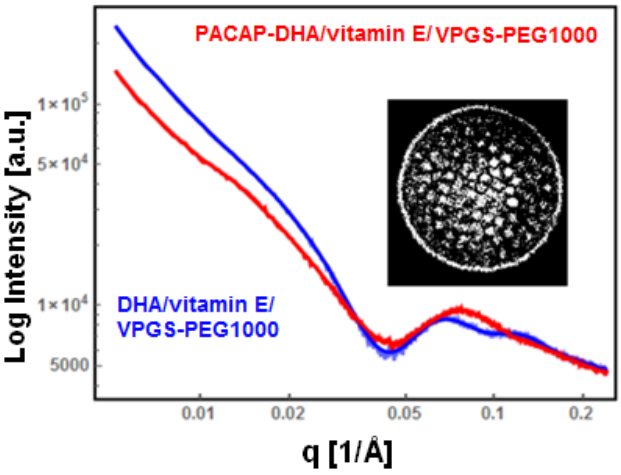

Figure 3. Synchrotron SAXS patterns of the lipidated peptide PACAP-DHA co-assembled in a PACAP-DHA/vitamin E/VPGS-PEG$_{1000}$ amphiphilic mixture (red plot). The PACAP-DHA concentration is 1 mg/ml for the sample volume. The blue plot corresponds to a mixed DHA/vitamin E/VPGS-PEG$_{1000}$ assembly (54/23/23 molar ratio) without a bound peptide PACAP. The latter is obtained upon functionalization of PEGylated VPGS-PEG$_{1000}$ (vitamin E α-tocopheryl polyethylene glycol 1000 succinate (VPGS-PEG$_{1000}$) micelles (3 mM concentration) by the lipid trophic factor DHA and vitamin E α-tocopherol. The two amphiphilic dispersions, shown by red and blue plots, are equivalently concentrated in DHA, vitamin E, and VPGS-PEG$_{1000}$. Temperature is 20 °C. Inset: Topology of the self-assembled core-shell structures deduced from a processed cryo-TEM image.

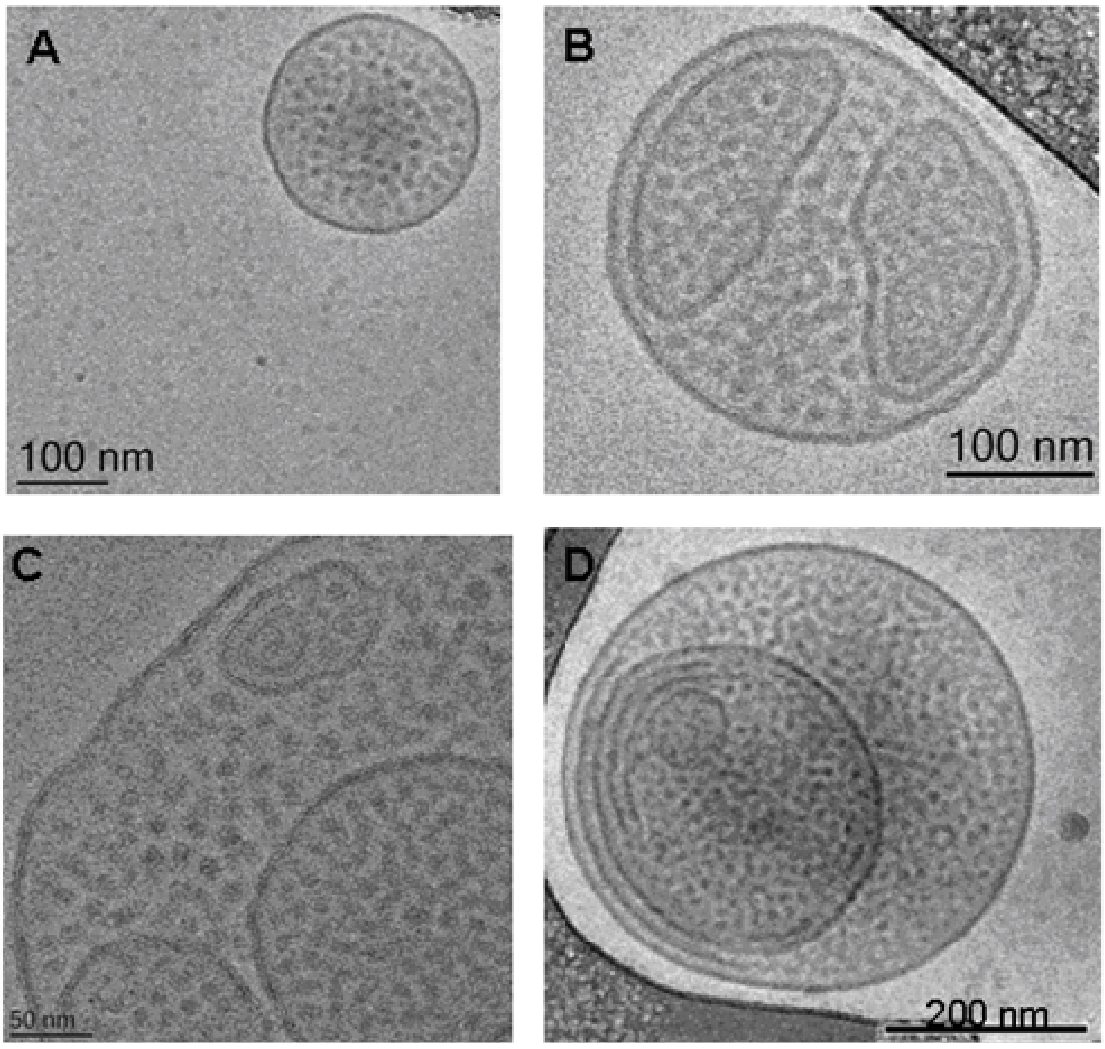

Figure 4. Cryo-TEM images of pep-lipid hierarchical assemblies with internal compartments: Membrane-mimetic environment of DHA/vitamin E/VPGS-PEG_{1000} assemblies (54/23/23 molar ratio) (A) into which the peptide PACAP is embedded at a concentration 4 mg/mL (B). (C,D) PACAP-DHA/vitamin E/VPGS-PEG_{1000} assemblies obtained at an equivalent molar ratio of the lipid components as in (A,B). The PACAP-DHA concentration is 1 mg/ml for the sample volume. The observed hierarchical organization comprises a coexistence of small micelles and compartmentalized vesicles (micello-vesicular containers). The generated vesicular membranes evolve to close shells that encapsulate small pep-lipid aggregates (D).

In the strategy to investigate the supramolecular assembly of multiple neuroprotective amphiphiles, we further proceeded with a BioSAXS study of the co-assembly of the PACAP-DHA peptide amphiphile with vitamin E in a membrane-like medium. The antioxidant vitamin E was chosen as a potential therapeutic compound in neuro-regeneration, suppression of oxidative stress and reduction of Aβ-amyloid peptide plaques in AD.[16b] Because the lipid building blocks DHA and Vitamin E are not water soluble, we used a micellar solution of the PEGylated agent (VPGS-PEG_{1000}: vitamin E α-tocopheryl polyethylene glycol 1000 succinate) for their solubilization. Bearing in mind the large molecular mass of the PACAP polypeptide (4.5 kDa) and its length in an extended state conformation (5.4 nm) (Fig. 1), the two lipophilic building blocks, DHA and vitamin E (Fig. 1), were required in order to create a bilayer membrane mimetic medium with an increased volume of the hydrophobic domain. The aim was to counterbalance the diminishment of the mean critical packing parameter[5a] of the pep-lipid system due to the presence of a large amino acid-sequence moiety. It is worth to note that the synthetic PACAP-DHA molecule has a net charge of +8 at pH 7.0-7.4, which augments its hydrosolubility with regard to a typical lipid-based prodrug.[8d] The proposed self-assembly approach is motivated by the fact that sterically-stabilized micelles involving polyethylene glycol (PEG) chains may amplify the bioactive properties of solubilized peptides.[16a]

The SAXS pattern of the PACAP-DHA/vitamin E/VPGS-PEG_{1000} self-assembled mixture is compared in Fig. 3 with that of dispersed DHA/vitamin E/VPGS-PEG_{1000} assemblies lacking a bound peptide hormone (red and blue plots). A coexistence of

particles (bimodal distribution) is detected upon the co-assembly of DHA and Vitamin E in the amphiphilic VPGS-PEG$_{1000}$ micellar medium. The dispersion of supramolecular amphiphilic aggregates of mixed compositions comprised larger nanoassemblies, which may correspond to vesicles. The created DHA/Vitamin E mixture, which behaves as a double chain amphiphile with a capacity for self-assembly into bilayer vesicle membranes.

We note that the SAXS curves in Fig. 3 considerably differ from that of PACAP-DHA alone (Fig. 2A) and also from that of

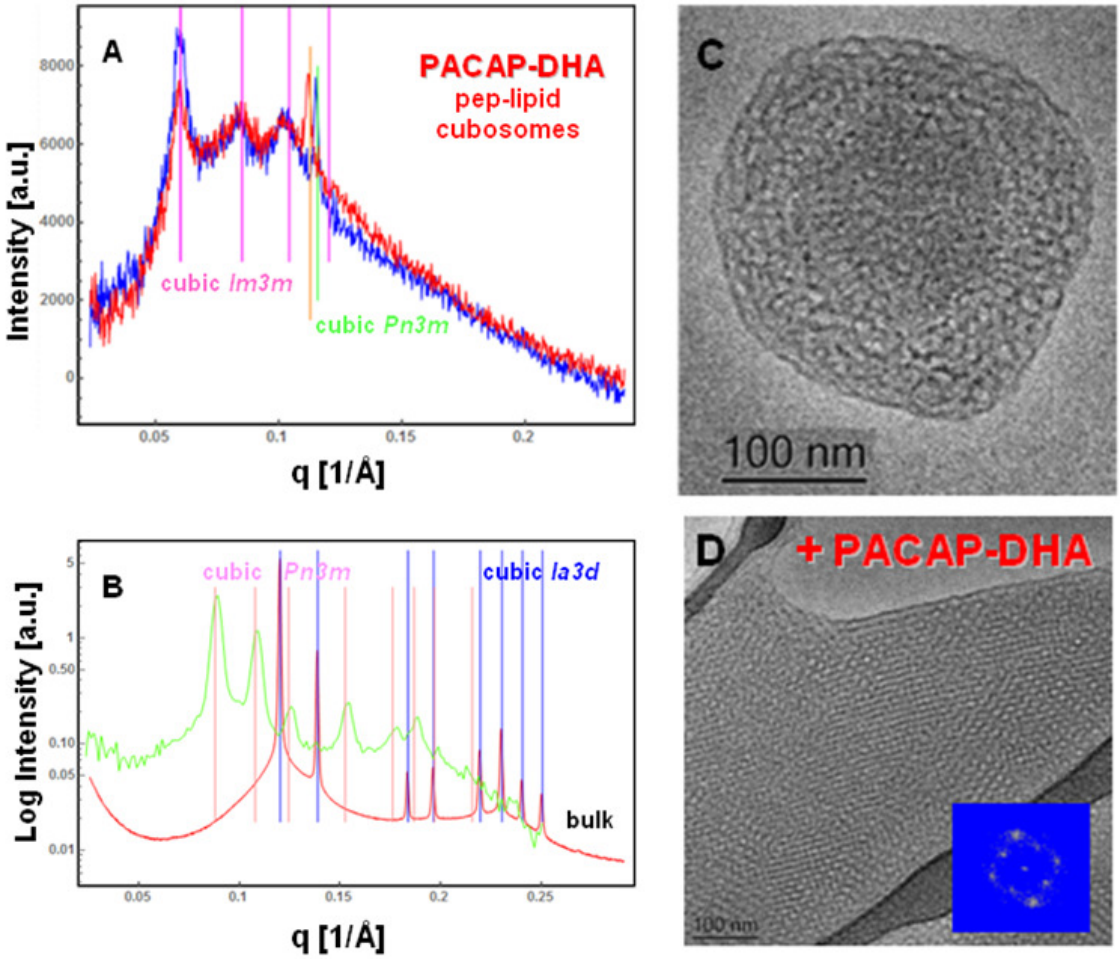

Figure 5. BioSAXS patterns of pep-lipid cubosomes. (A) Cubosome nanodispersions obtained at full hydration (95 wt.% aqueous phase). The PACAP-DHA is embedded in a nanochanneled network formed by the MO/DHA/vitamin E/VPGS-PEG$_{1000}$ cubic-phase mixture (lipid molar ratio 69/18/9/4) in excess aqueous phase. The red plot corresponds to the pep-lipid composition PACAP-DHA/MO/DHA/vitamin E/VPGS-PEG$_{1000}$, whereas the blue plot refers to the MO/DHA/vitamin E/VPGS-PEG$_{1000}$ assemblies. The molar fraction of the PACAP-DHA is 1/50 with regard to the DHA lipid. The PACAP-DHA concentration is 1 mg/ml for the sample volume. The detected Bragg peaks evidenced the formation of cubosomes of *Im3m* inner cubic symmetry. (B) SAXS patterns of bulk monoolein cubic phases formed at two different hydration levels [80 wt.% (green plot) and 40 wt.% (red plot) aqueous phase]. The sequence of Bragg peaks spaced in the ratio $\sqrt{2} : \sqrt{3} : \sqrt{4} : \sqrt{6} : \sqrt{8} : \sqrt{9} : \sqrt{10} : \sqrt{11}$ is characteristic of a bicontinuous *Pn3m* double diamond cubic lattice, whereas the sequence of Bragg peaks spaced in the ratio $\sqrt{6} : \sqrt{8} : \sqrt{14} : \sqrt{16} : \sqrt{20} : \sqrt{22} : \sqrt{24} : \sqrt{26}$ defines a gyroid *Ia3d* cubic lattice. Temperature is 20 °C. (C,D) Cryo-TEM images of pep-lipid cubosomes involving PACAP-DHA macromolecules. (C) A small cubosome particle of a PACAP-DHA/MO/DHA/vitamin E/VPGS-PEG$_{1000}$ composition preserving the inner cubic structure upon dispersion from the bulk liquid crystalline phase. (D) A cubosome carrier of PACAP-DHA (lipid molar ratio as in (A)), for which the Stealth shell is invisible at the nanoparticle periphery due to the insufficient electron density contrast of the PEG chains. The Fast Fourier Transform (FFT) pattern (inset) derived from the cryo-TEM image reveals the *Im3m* inner cubic membrane organization of the pep-lipid cubosomes.

new nanoparticles are bigger in size (diameters above 100 nm) as compared to the initially monodispersed PEGylated micelles (VPGS-PEG$_{1000}$) of a mean diameter d=11 nm determined at the studied concentration of 3 mM. It should be emphasized that the presence of both DHA and Vitamin E building blocks is required to form vesicle bilayer assemblies in the studied system. Vitamin E alone does not induce the formation of vesicular membranes upon solubilization in VPGS-PEG$_{1000}$ micelles. It is the the VPGS-PEG$_{1000}$ surfactant micelles (Fig. S1). This reveals the structural change triggered by the pep-lipid co-assembly with DHA and vitamin E. The formation of stable PEGylated amphiphilic dispersions evidenced the preference of PACAP-DHA for encapsulation in a membrane mimetic environment.

Topological features of pep-lipid supramolecular aggregates PACAP-DHA/vitamin E/VPGS-PEG$_{1000}$

The topological features of the spontaneously self-assembled PEGylated pep-lipid aggregates (PACAP-DHA/vitamin E/VPGS-PEG_{1000}) were directly visualized by cryo-TEM imaging. Figure 4 revealed the induction of new multicompartment supramolecular structures in the PACAP-DHA/vitamin E/VPGS-PEG_{1000} dispersions and the coexistence of small and larger-size nanoassemblies. As in the SAXS experiments, DHA was employed both as a pure lipid and in its bound state to the PACAP ligand. The lipid DHA/vitamin E/VPGS-PEG_{1000} nanocarriers formed vesicle-like shells at a DHA content equivalent to that in the PACAP-DHA-containing amphiphilic mixtures (the sample concentrations are the same as those measured by SAXS in Fig. 3). These structures likely result from the bilayer membrane-type packing of the DHA, PACAP-DHA and vitamin E components. We suggest that the single-chain DHA lipid associates with vitamin E in the shape of a double-chain amphiphile, which forms bilayer vesicles. Coexisting small spherical and elongated nanoparticles were found to be encapsulated in bigger closed-bilayer shells. Such structures were observed by cryo-TEM imaging before and after the inclusion of PACAP polypeptide chains as building blocks of the supramolecular assemblies. The observed hybrid morphologies (Fig. 4) corroborate with the occurrence of a structural transition, which was evidenced by the BioSAXS analysis.

Small micellar aggregates were found to occupy variable fractions of the projected planes in the cryo-TEM images as they get modified by the PACAP polypeptide chain (Fig. 4B,C). The high resolution micrographs demonstrate the development of compartmentalized supramolecular architectures characterized by intriguing patterns (Fig. 4B,C). They reveal the formation of compartmentalized vesicles (micello-vesicular containers) starting from lipid bilayer membrane fragments and shells. The vesicular reservoirs displayed mean diameters in the range from 150 nm to 350 nm.

A closer inspection of the images in Figure 4 by the *Image J* software (National Institutes of Health) established that the spatial arrangement in the compartmentalized amphiphilic aggregates represents a network packing of small objects insides the vesicular reservoirs of mixed amphiphilic compositions (see the inset in Fig. 3). The achievement of the hybrid micello-vesicular organization appears to be preceded by curvature changes and fusion of the spherical micelles into more extended structures. This favors the development of flexible amphiphile/water interfaces, which may transform the vesicular membranes into closed containers (Fig. 4D).

The compact patterns in Figure 4 resemble projections of a network of pep-lipid micelles, which are encapsulated in vesicular membrane shells stabilized by PEG chains. The stabilization of the built-up interesting cytoskeleton-like patterns (Figure 4) may be due to the formation of electrostatic bridges between the charged residues of the peptide amphiphile PACAP-DHA and the carboxylic headgroups of the lipid DHA in the nanocarriers formed at pH 7.0. Hydrophobic attraction forces between the non-charged regions of the peptide sequences may also contribute to the assembly of neighbouring pep-lipid micelles inside bigger pep-lipid shells. We suggest that these soft nanoarchitectures can provide enhanced drug content for therapeutic innovation purposes through sustained release properties.

The induced self-assembled pep-lipid nanostructures in the present work are different from vesosomes (vesicles with inner organization of encapsulated small vesicles) or stomatosomes (perforated bilayer vesicles) produced by particular lipid and surfactant systems.[21] They are referred to as compartmentalized bilayer vesicle embedding pep-lipid micelles. We are not aware of literature reports on such compartmentalized hybrid patterns in other pep-lipid assemblies.

Cubic-phase liquid crystalline nanocarriers (cubosomes) embedding the large peptide hormone PACAP-DHA

In a further step, the lipidated peptide PACAP-DHA was expected to show affinity for incorporation in lipid membranous assemblies, which can stabilize the peptide conformation as in native membranous systems.[16] Cubosome reservoirs with distinct internal hydrophobic and hydrophilic compartments are highly efficient for peptide and protein nanoformulation.[17,18] A nanostructured liquid crystalline membrane medium was created using cubic-phase assemblies of the hydrated nonlamellar lipid monoolein (MO).[17-19] The lipid trophic factor DHA and vitamin E (α-tocopherol) were included towards functionalization of the cubic phase matrix by neuroprotective molecules. For steric stabilization of the cubosomes, PEGylation was realized by the inclusion of VPGS-PEG_{1000}. The presented structural results in Figure 5 refer to the incorporation of the peptide amphiphile PACAP-DHA in MO/DHA/vitamin E/VPGS-PEG_{1000} mixed nanoassemblies of a lipid molar ratio 69/18/9/4. Nanoparticle dispersions are obtained at lipid/water weight ratio 5/95 wt./wt.

The SAXS patterns in Figure 5A characterize highly hydrated cubosome particles PACAP-DHA/MO/DHA/vitamin E/VPGS-PEG_{1000} dispersed in an excess aqueous phase. Liquid crystalline structures with inner cubic lattice periodicities (cubosomes) are evident before and after the incorporation of the lipidated hormone PACAP-DHA.

Pep-lipid supramolecular assemblies (PACAP-DHA/MO/DHA/vitamin E/VPGS-PEG_{1000}) of a cubic phase nanochannel network organization (pep-lipid cubosomes) were obtained at a molar ratio of 1:50 between the PACAP-DHA and the DHA lipid in the nanocarriers (Figure 5A). Under these conditions, we established that the inner cubic structure of the nanoparticulate assemblies (cubosomes) remains stable in the presence of the modified PACAP-DHA peptide hormone. The sequence of Bragg peak positions spaced in the ratio $\sqrt{2} : \sqrt{4} : \sqrt{6}$, and having a first peak at q =0.104 $Å^{-1}$, identified a primitive *Im3m* inner cubic lattice structure of the PEGylated cubosomes. The unit cell dimension was determined to be a_{Im3m} =14.7 nm for both the PACAP-DHA/MO/DHA/vitamin E/VPGS-PEG_{1000} and the MO/DHA/vitamin E/VPGS-PEG_{1000} cubosomes at a lipid molar ratio 69/18/9/4. Thus, the dominant inner structure of the PEGylated cubosomes was of the primitive *Im3m* inner cubic lattice space group for the PACAP-DHA loaded nanocarriers.

An additional Bragg peak was observed at q=0.11 $Å^{-1}$ (Figure 5A). It was attributed to incompletely PEGylated lipid cubic membrane domains based on knowledge from our previous work.[19b] Such domains keep the bicontinuous diamond (*Pn3m*) cubic structure of the non-PEGylated lipid cubic

membrane located in the core of the cubosome particles. The cubic unit cell sizes are a_{Pn3m} =11.1 nm (orange bar, PACAP-DHA/MO/DHA/vitamin E/VPGS-PEG$_{1000}$ cubosomes) and a_{Pn3m} =10.8 nm (green bar, MO/DHA/vitamin E/VPGS-PEG$_{1000}$ cubosomes), respectively. Alternatively, a coexisting minor fraction of onion-lamellar-phase particles may explain the peaks observed at q=0.11 Å^{-1}. The latter might correspond to a first-order Bragg reflection of a minor lamellar phase yielding repeat spacing of 5.56 nm (orange bar) or 5.42 nm (green bar).

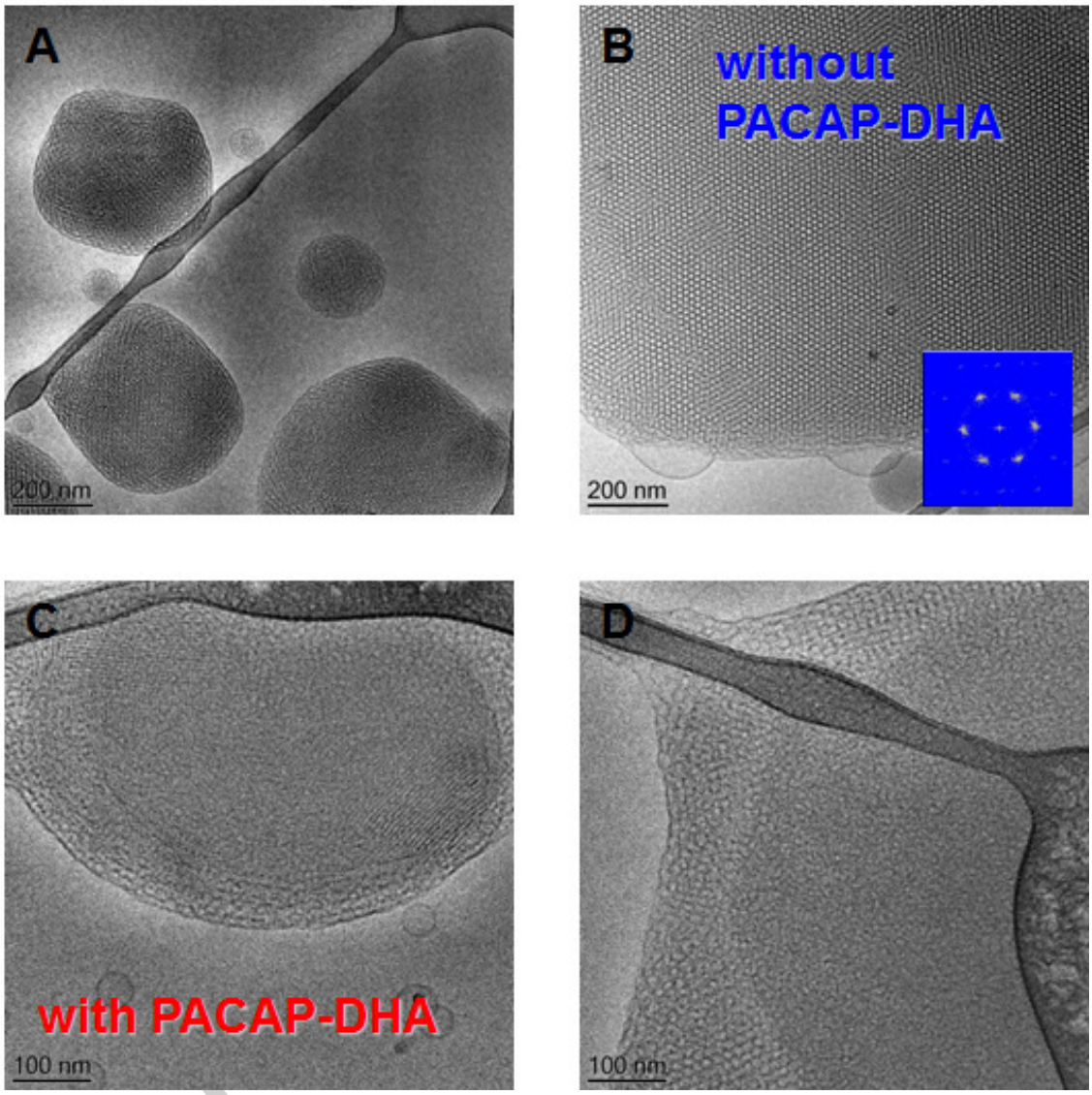

Figure 6. Cryo-TEM images of cubosomes with multiple functionalities: MO/DHA/vitamin E/VPGS-PEG$_{1000}$ nanoassemblies (lipid molar ratio 69/18/9/4) before (A,B) and after (C,D) the inclusion of PACAP-DHA. The pep-lipid cubosomes are prepared at a molar ratio 1:50 between PACAP-DHA and DHA. Inset: A Fast Fourier Transform (FFT) pattern derived from the cryo-TEM image in Fig. 6B.

The SAXS patterns of the bulk MO cubic phases acquired at two hydration levels (80 wt.% and 40 wt.% aqueous phase) are shown in Figure 5B. The obtained sets of Bragg peaks are characteristic of well-ordered liquid crystalline cubic organizations of the nonlamellar lipid matrix. They show that the diminished hydration level leads to a transformation of the bicontinuous double diamond (*Pn3m* crystallographic space group) cubic structure (observed at 80 wt.% aqueous content) into a bicontinuous gyroid (*Ia3d* space group) cubic phase (observed at 40 wt.% aqueous content). The cubic unit cell dimensions are dependent on the hydration level (a_{Pn3m} = 10.1 nm and a_{Ia3d} = 12.8 nm, respectively) in accordance with the MO lipid phase behavior.

Taking into account the experimentally determined unit cell sizes of the bulk lipid cubic phases (Fig. 5B), it is evident that the obtained novel pep-lipid cubosomes comprise swollen-type membranous architectures (Fig. 5A). The encapsulated PACAP-DHA peptide amphiphile did not cause dehydration of the inner nanochannel network structure of the cubosome particles (a_{Im3m} = 14.7 nm).

Topological features of pep-lipid cubosomes

The topological features of the pep-lipid cubosomes PACAP-DHA/MO/DHA/vitamin E/VPGS-PEG_{1000} and MO/DHA/vitamin E/VPGS-PEG_{1000} (lipid molar ratio 69/18/9/4) were further characterized by cryo-TEM imaging. The micrographs of the multicomponent nanoparticulate assemblies presented in Figure 6 demonstrate that 3D cubic membrane architectures are predominantly present. This finding is in accordance with the obtained BioSAXS results (Fig. 5A). Under the investigated experimental conditions, the PACAP-DHA did not induce the formation of a lamellar layered structure as a major phase. As a consequence, the Bragg peak at q =0.113 $Å^{-1}$ can be indexed as a first order reflection of a minor fraction of a *Pn3m* lipid cubic structure, for which the higher order Bragg peaks remain weak. The latter are visually overlapped by the scattering of the prevailing *Im3m* cubic phase (Fig. 5A).

The inclusion of the peptide amphiphile PACAP-DHA in the self-assembled mixture led to certain morphological changes in the host membrane system (Fig. 6C,D). This structural effect confirmed the encapsulation of PACAP-DHA in the host lipid nanocarriers.

A core-shell organization is apparent for the pep-lipid cubosomes shown in Fig. 6(C,D). The peripheries of the cubosomes comprise swollen nanochannels (Fig. 6D). At variance, the core of the big cubosome particles exhibits a more dense texture of nanochannels (Fig. 6C). The fast Fourier Transform (FFT) pattern of the cryo-TEM image confirmed the cubic lattice periodicity. The resulting hexagonal section corresponds to the projection of the (111) crystallographic plane of the diamond type cubic lattice domain. This organization is generated in cubic domains of large sizes and corresponds to a low degree of PEGylation of the lipid/water interfaces.[19b]

Figure 5C shows a cryo-TEM image of a small-size pep-lipid cubosome of the PACAP-DHA/MO/DHA/vitamin E/VPGS-PEG_{1000} composition, in which the lipid/water interfaces play a more significant role. The perturbation of the cubic lattice order owing to the insertion of the peptide amphiphile PACAP-DHA in the lipidic cubic lattice network is more essential. The Fast Fourier Transform (FFT) pattern of the image in Fig. 5D evidences a cubic lattice of the primitive *Im3m* space group. The latter corroborates with the BioSAXS results (Fig. 5A), which deduced a predominant cubic *Im3m* organization of the cubosomes.

The structural features of the obtained PACAP-DHA cubosomes can be compared with those established upon building of nanoscale assemblies by other large cationic peptides. For instance, the cationic brain-derived neurotrophic factor (BDNF), characterized by β-sheet peptide conformation, has been shown to induce the formation of cubic lattice domains and multicompartment organizations in lipid membranous assemblies containing eicosapentaenoic acid (EPA, w-3 C20:5).[1c] At variance, the PACAP-DHA peptide amphiphile showed a tendency towards distortion of the long-range liquid crystalline order of the host cubic membrane matrices (Figure 6). This may be due to partial insertion of the helical peptide moieties in the interfacial lipid headgroup/water regions and altering of the lateral lipid membrane packing in the nanoassemblies.

Despite of the reported variety of nanoparticulate assemblies of liquid crystalline order and hierarchical complexity[5-7,9,19c], the investigations in which the structural organization of the lipid nanocarriers has been suggested as beneficial for curing of neurodegenerative disorders are scarce.[1c,7b,10a,13b,13c,17a] The modifications of GPCR ligands and other neuropeptides by lipophilic anchors is suggested as a possibility for enhancement of the neuropeptide drug bioavailability. The proposed here multilevel assembly of bioactive building blocks into nanocarriers represents a step forward the development of disease-modifying drug delivery systems for neurological disorders. The double-ligand PACAP-DHA bioactive conjugate was embedded in liquid crystalline nanocarriers, which were stably dispersed as PEGylated particles. The cryo-TEM and BioSAXS analyses suggested that the new pep-lipid scaffolds of hierarchical organizations can be employed in sustained drug-release applications. A slow release modality can be expected thanks to the multi-compartment structure of the generated hybrid micello-vesicular containers. In addition, PEGylation (by varying amounts of the PEGylated amphiphile) may provide increased half-life of the nanoassemblies. All these structural features should contribute to the spatial and temporal regulation of the material transport in the compartmentalized structures, and in particular, of the peptide drug release from the nanocarriers.

The obtained internally nanostructured pep-lipid carriers comprise periodically organized labyrinthine patterns of aqueous nanochannels (cubosomes) (Fig. 6). The realization of channels swelling and gating through alteration of the channels diameter and variation of the nanochannels density is of technological importance for the design of “breathing” soft nanomaterials. Indeed, mesoporous cubic lattice architectures present strong current interest in a number of scientific fields.[5-7,11,18-20] It is remarkable that the observed organized ladybird-like patterns with internal compartments as well as the periodic cubic lipid membrane structures (Fig. 6) mimic the biological compartmentalization in living systems.[22] On the other hand, the organizational complexity of the scaffolds involving the lipidated high-molecular weight peptide hormone is beyond the one that has been reached with small lipid-like peptide surfactants.[23,24]

Conclusions

Our purpose in this work was to create and reveal the structure of neuroprotective pep-lipid assemblies stabilized in membrane-mimetic environment in contact with aqueous surrounding. The acquired synchrotron small-angle X-ray scattering (BioSAXS) patterns of the native pituitary adenylate

cyclase-activating polypeptide (PACAP) and the lipidated peptide PACAP-DHA were used for deduction of structural information about their self-assembly properties in supramolecular aggregates. Despite that the large peptide amphiphile PACAP-DHA can form alone self-assembled nanoparticles, in our opinion it requires protective nanocarriers for transport and prolonged delivery in biological media. The employed membrane building blocks spontaneously co-assembled with PACAP-DHA into intriguing compartmentalized architectures (vesicles embedding pep-lipid micelles and pep-lipid cubosomes with functionalized lipid bilayer interfaces) that are expected to increase the bioavailabilty of the studied class-B GPCR ligand. We are not aware of other synthetic pep-lipid assemblies of such sophisticated hierarchical topologies. Moreover, the incorporation of two neurotrophic factors in multicompartment nanocarriers is expected to be advantageous for combination therapy strategies in nanomedicine of neurodegenerative disorders.

Experimental Section

Materials and samples preparation

Cis-4,7,10,13,16,19-docosahexaenoic acid (DHA) (MW 328.49, purity ≥ 98%), 1-oleoyl-rac-glycerol (MO) (MW 356.55, purity ≥99.5%), vitamin E α-tocopherol (MW 430.71, Eur Pharmacopeia grade), vitamin E D-α-tocopheryl polyethylene glycol 1000 succinate (VPGS-PEG_{1000}) (MW 1513, BioXtra), butylated hydroxytoluene (BHT), and D-(+)-glucose (BioReagent) were purchased from Sigma-Aldrich (Saint Quentin). The peptide PACAP composed of 38 aminoacid residues (PACAP-38, NH2-HSDGIFTDSYSRYRKQMAVKKYLAAVLGKRYKQRVKNK-COOH) was custom synthesized by ChinaPeptides Ltd. (Shanghai). Its purity was 95.34%. The C-terminal Lys-38 residue of the PACAP-38 peptide sequence was modified by cis-4,7,10,13,16,19-docosahexaenoic acid (DHA), which yielded the synthetic peptide amphiphile PACAP-DHA. Its purity was 97.54% according to the specifications from the supplier. Both peptides, produced and certified by ISO9001 at ChinaPeptides Ltd., were delivered for research purposes as lyophilized powders of trifluoroacetate salts. The determined molecular weights in the material datasheets of the products were consistent with the theoretical molecular masses of PACAP-38 (4534.3) and its conjugate with DHA (MW 328.49). The experimental molecular weights of 4.54 kDa (PACAP) and 4.86 kDa (PACAP-DHA) we used, respectively. Aqueous solutions were prepared using MilliQ water of resistivity 18.2 MΩ.cm (Millipore Co.). The MilliQ water was saturated in BHT antioxidant. The pH value was controlled using 0.01 M phosphate buffers.

The method for preparation of dispersions of nanoassemblies by hydration of lyophilized mixed lipid films is analogous to the previously described.[20] In brief, the experimental procedure involved a step of mixing of the lipid components in chloroform at desired ratios and evaporation of the organic solvent under a gentle stream of nitrogen gas . The obtained homogeneous lipid films were lyophilized overnight. The hydration of the mixed lipid layers was done upon incubation with an aqueous phase (pH 7.0) containing BHT. The hydration, vortexing and agitation of the prepared mixed amphiphilic films were performed in an excess buffer medium for nanoparticles preparation. Bulk lipid phases were self-assembled in 40 wt.% and 80 wt.% aqueous phase *(i.e.* lipid/water weight ratios 60/40 wt./wt. and 80/20 wt./wt.), whereas nanoparticulate dispersions were obtained with 95wt.% excess aqueous phase content (*i.e.* lipid/water weight ratio 5/95 wt./wt.). The dispersion of the PACAP-DHA/vitamin E/VPGS-PEG_{1000} and DHA/vitamin E/VPGS-PEG_{1000} self-assembled mixtures into nanoparticles was spontaneous and did not required ultrasonication. An ultrasonic bath (Branson 2510 ultrasonic bath, "set sonics" mode, power 60W) was used for dispersion of the MO-containing lipid mixtures. The presented here ratios between the amphiphilic components were determined in preliminary experiments.

Biological small-angle X-ray scattering (BioSAXS)

Synchrotron BioSAXS experiments were performed at the P12 BioSAXS beamline of the European Molecular Biology Laboratory (EMBL) at the storage ring PETRA III of the Deutsche Elektronen Synchrotron (DESY, Hamburg, Germany) at 20 °C using synchrotron radiation with a wavelength λ = 1 Å and a Pilatus 2M detector (1475 x 1679 pixels) (Dectris, Switzerland). The pixel size was 172 x 172 mm^2. The sample-to-detector distance was 3 m, and the accessible q-range from 0.005 to 0.35 $Å^{-1}$. The *q*-vector was defined as $q = (4\pi/\lambda) \sin\theta$, where 2θ is the scattering angle. The q-range was calibrated using the diffraction patterns of silver behenate. The experimental data were normalized with respect to the incident beam intensity. The background scattering of the quartz capillary and the aqueous solvent was subtracted. The solvent scattering was measured before and after every sample. Twenty consecutive frames (each 0.05s) comprising the measurements for the sample and the solvent were acquired. No measurable radiation damage was detected by the comparison of the successive time frames. An automatic sample changer adjusted for sample volume of 20 µL and a filling cycle of 1 min was used. The condensed phase samples were filled in 1.5 mm diameter capillaries, which were measured consecutively. The ATSAS analysis software[25a] was used in BioSAXS data treatment.[25]

Cryogenic Transmission Electron Microscopy (Cryo-TEM)

For Cryo-TEM imaging, liquid samples (2 µL) were dropped on a lacey carbon film covered copper grid (Science Services, Munich, Germany), which was hydrophilized by glow discharge for 15 s. The thin film specimens were instantly shock frozen by rapid immersion into liquid ethane and cooled to approximately 90 K by liquid nitrogen in a temperature-controlled freezing unit (Zeiss Cryobox, Zeiss NTS GmbH, Oberkochen, Germany). After removing ethane, the frozen samples were inserted into a cryo transfer holder (CT3500, Gatan, Munich, Germany) and transferred to a Zeiss EM922 Omega energy-filtered TEM (EFTEM) instrument (Zeiss NTS GmbH, Oberkochen, Germany). The imaging studies were carried out at temperatures around 90 K. The TEM instrument was operated at an acceleration voltage of 200 kV. Zero-loss-filtered images (ΔE = 0 eV) were taken under reduced dose conditions (100-1000 e/nm^2). The images were recorded digitally by a bottom-mounted charge-coupled device (CCD) camera system (Ultra Scan 1000, Gatan, Munich, Germany) and combined and processed with a digital imaging processing system (Digital Micrograph GMS 1.8, Gatan, Munich, Germany).

Acknowledgements

The project support No.17-00973S of GACR (Czech Science Foundation) and ELIOBIO "Structural dynamics of biomolecular systems" (CZ.02.1.01/0.0/0.0/15_003/0000447) from the European Regional Development Fund is acknowledged by B.A. M.D. is supported by the SFB840 collaborative research centre of DFG. We thank Dr. C.E. Blanchet for the assistance at the EMBL BioSAXS beamline P12 at Petra III (Hamburg, Germany).

Keywords: BioSAXS ; cryo-TEM ; cubosome ; lipidated peptide hormone (class B GPCR ligand) ; multicompartment nanostructure

[1] (a) K. Liu, R. Xing, Q. Zou, G. Ma, H. Möhwald, X. Yan, *Angew. Chem. Int. Ed.* **2016**, *55*, 3036-3039. (b) X. Yan, Q. He, K. Wang, L. Duan, Y. Cui, J. Li, *Angew Chem Int Ed* **2007**, *46,* 2431-4. (c) B. Angelov, A. Angelova, S.K. Filippov, M. Drechsler, P. Štěpánek, S. Lesieur, *ACS Nano*, **2014**, *8*, 5216-5226.

[2] (a) M. Dwivedi, T. Mejuch, H. Waldmann, R. Winter, *Angew. Chem. Int. Ed.* **2017**, *56*, 10511-10515. (b) A. Vogel, G. Reuter, K. Weise, G. Triola, J. Nikolaus, K.-T. Tan, C. Nowak, A. Herrmann, H. Waldmann, R. Winter, D. Huster, *Angew. Chem. Int. Ed.* **2009**, *48*, 8784-8787.

[3] (a) K. Kornmueller, B. Lehofer, G. Leitinger, H. Amenitsch, R. Prassl, *Nano Res.* **2018**, *11*, 913-928. (b) R. Oliva, P. del Vecchio, A. Grimaldi, E. Notomista, V. Cafaro, K. Pane, V. Schuabb, R. Winter, L. Petraccone, *Phys. Chem. Chem. Phys.* **2019**, *21*, 3989-3998. (c) K. Sato, M.P. Hendricks, L.C. Palmer, S.I. Stupp, *Chem Soc Rev.* **2018**, *47*, 7539-7551.

[4] (a) F. Thomas, N.C. Burgess, A.R. Thomson, D.N. Woolfson, *Angew. Chem. Int. Ed.*, **2016**, *55*, 987-991. (b) M. Li, M. Radic Stojkovic, M. Ehlers, E. Zellermann, I. Piantanida, C. Schmuck, *Angew. Chem. Int. Ed,* **2016**, *55*, 13015-13018.

[5] (a) A. Yaghmur, B. Sartori, M. Rappolt, *Langmuir*, **2012**, *28*, 10105-119. (b) B. Angelov, V.M. Garamus, M. Drechsler, A. Angelova, *J. Mol. Liquids*, **2017**, *235*, 83-89. (c) A. Yaghmur, M. Rappolt, S.W. Larsen, *J. Drug Delivery Sci. Tech.* **2013**, *23*, 325-332.

[6] (a) A. Angelova, B. Angelov, R. Mutafchieva, S. Lesieur, P. Couvreur, *Acc. Chem. Res.,* **2011**, *44*, 147–156. (b) S. Aleandri, C. Speziale, R. Mezzenga, E.M. Landau, *Langmuir* **2015**, *31*, 6981–6987.

[7] (a) M. Fu, Q. Li, B. Sun, Y. Yang, L. Dai, T. Nylander, J. Li, *ACS Nano* **2017**, *11*, 7349-7354. (b) A. Angelova, B. Angelov, M. Drechsler, S. Lesieur, *Drug Discovery Today*, **2013**, *18*, 1263–1271. (c) H. Azhari, M. Strauss, S. Hook, B.J. Boyd, S.B. Rizwan, *Eur J Pharm Biopharm,* **2016**, *104*, 148–55.

[8] (a) H.X. Wang, H.Y.; Xie, J.G. Wang, J. Wu, X. Ma, L. Li , X. Wei, Q. Ling, P. Song, L. Zhou, X. Xu, S. Zheng, *Adv. Functional Materials* **2015**, *25*, 4956–4965. (b) J. Zhai, T.M. Hinton, L.J. Waddington, C. Fong, N. Tran, X. Mulet, C.J. Drummond, B.W. Muir, *Langmuir*, **2015,** *31*, 10871-10880. (c) D. Irby, C. Du, F. Li, *Mol Pharm.* **2017**, *14*, 1325-1338. (d) X. Gong, M.J. Moghaddam, S.M. Sagnella, C.E. Conn, S.J. Danon, L.J. Waddington, C.J. Drummond, *Colloids Surf. B,* **2011**, *85*, 349–59.

[9] (a) P. Couvreur, L.H. Reddy, S. Mangenot, J.H. Poupaert, D. Desmaële, S. Lepêtre-Mouelhi, B. Pili, C. Bourgaux, H. Amenitsch, M. Ollivon,. *Small* **2008**, *4*, 247– 253. (b) J.A. Hutchinson, S. Burholt, I.W. Hamley, *J. Peptide Sci.* **2017**, *23*, 82–94. (c) Q. Liu, J. Wang, Y.D. Dong, B.J. Boyd, *J. Colloid Interface Sci.* **2015**, *449*, 122-129. (d) S. P. Akhlaghi, W. Loh, *Eur J Pharm Biopharm.* **2017**, *117*, 60-67.

[10] (a) V. Castelletto, P. Ryumin, R. Cramer, I.W. Hamley, M. Taylor, D. Allsop, M. Reza, J. Ruokolainen, T. Arnold, D. Hermida-Merino, C. I. Garcia, M. C. Leal, E. Castaño, *Sci. Rep.* **2017***, 7*, 43637; (b) A.N. Edelbrock, Z. Àlvarez, D. Simkin, T. Fyrner, S.M. Chin, K. Sato, E. Kiskinis, S.I. Stupp, *Nano Lett.,* **2018,** *18*, 6237-6247; (c) R. Liu, G.A. Hudalla, *Molecules,* **2019***, 24*, 1450.

[11] (a) L. Boge, K. Hallstensson, L. Ringstad, J. Johansson, T. Andersson, M. Davoudi, P.T. Larsson, M. Mahlapuu, J. Håkansson, M. Andersson, *Eur. J. Pharm. Biopharm.* **2019***, 134*, 60-67; (b) L. Boge, A. Umerska, N. Matougui, H. Bysell, L. Ringstad, M. Davoudi, J. Eriksson, K. Edwards, M. Andersson, *Int J. Pharm.* **2017***, 526*, 400-412; (c) L. Boge, H. Bysell, L. Ringstad, D. Wennman, A. Umerska, V. Cassisa, J. Eriksson, M.-L. Joly-Guillou, K. Edwards, M. Andersson, *Langmuir* **2016***, 32*, 4217-4228; (d) I.D.M. Azmi, S.M. Moghimi, A. Yaghmur, *Ther. Deliv.,* **2015***, 6*, 1347-1364.

[12] (a) H. Wang, X.X. Zhao, L.L. Li, Y. Zhao, H.W. An, Q. Cai, J.-Y. Lang, X.-X. Han, B. Peng, Y. Fei, H. Liu, H. Qin, G. Nie, *Angew Chem Int Ed*, **2019**, DOI: 10.1002/anie.201908185; (b) A. Angelova, R. Ianev, M.H.J. Koch, G. Rapp, *Archives Biochem. Biophys.,* **2000***, 378*, 93-106; (c) R. Fan, L. Mei, X. Gao, Y. Wang, M. Xiang, Y. Zheng, A. Tong, X. Zhang, B. Han, L. Zhou, P. Mi, C. You, Z. Qian, Y. Wei, G. Guo, *Adv Sci. (Weinh).* **2017***, 4*, 1600285. (d) D. Liu, A. Angelova, J. Liu, V.M. Garamus, B. Angelov, X. Zhang, Y. Li, G. Feger, N. Li, A. Zou, *J. Mater. Chem B.* **2019***, 7*, 4706-4716.

[13] (a) B. Lu, G. Nagappan, X. Guan, P.J. Nathan, P. Wren, *Nat. Rev. Neurosci.* **2013**, *14*, 401-416. (b) A. Angelova, B. Angelov, *Neural Neural Regener. Res.*, **2017**, *12*, 886-889. (c) R. Pangeni, S. Sharma, G. Mustafa, A. Javed, S. Baboota,. *Nanotechnology*, **2014**, *25*, 485102.

[14] a) I. Lauritzen, N. Blondeau, C. Heurteaux, C. Widmann, G. Romey, M. Lazdunski,. *The EMBO J.* **2000**, *19*, 1784–1793. (b) S.R. Shaikh, J.J. Kinnun, X. Leng, J.A. Williams, S.R. Wassall, *Biochim. Biophys. Acta-Biomembranes* **2015**, *1848*, 211-219. (c) B. Angelov, A. Angelova, *Nanoscale*, **2017**, *9*, 9797-9804.

[15] (a) T. Seaborn, O. Masmoudi-Kouli, A. Fournier, H. Vaudry, O. Vaudry,. *Curr Pharm Des.* **2011**, *17*, 204-214. (b) D. Vaudry, A. Falluel-Morel, S. Bourgault, M. Basille, D. Burel, O. Wurtz, A. Fournier, B.K. Chow, H. Hashimoto, L. Galas, H. Vaudry, *Pharmacol Rev.* **2009**, *61*, 283-357. (c) R. Yang, X. Jiang, R. Ji, L. Meng, F. Liu, X. Chen, Y. Xin, *Cell Mol Biol Lett.* **2015**, *20*, 265-278. (d) D. Reglodi, P. Kiss, A. Lubics, A.; Tams, *Curr Pharm Des.* **2011**, *17*, 962-972.

[16] (a) C. Sun, D. Song, R.A. Davis-Taber, L.W. Barrett, V.E. Scott, P.L. Richardson, A. Pereda-Lopez, M.E. Uchic, L.R. Solomon, M.R. Lake, K.A. Walter, P.J. Hajduk, E.T. Olejniczak, *Proc Natl Acad Sci USA.* **2007**, *104*, 7875–7880. (b) F. Osakada, A. Hashino, T. Kume, H. Katsuki, S. Kaneko, A. Akaike, *Neuropharmacology*. **2004**, *47*, 904-915.

[17] (a) M. Rakotoarisoa, B. Angelov, V.M. Garamus, A. Angelova, *ACS Omega*, **2019***, 4*, 3061-3073; (b) L.P.B. Guerzoni, V. Nicolas, A. Angelova, *Pharm. Res.* **2017**, *34*, 492–505. (c) A. Angelova, M. Ollivon, A. Campitelli, C. Bourgaux, *Langmuir*, **2003**, *19*, 6928 –6935.

[18] (a) A. Angelova, A.; Angelov, B.; Garamus, V.M.; Couvreur, P.; Lesieur, S. *J. Phys. Chem. Lett.*, **2012**, *3*, 445-457. (b) A. Angelova, B. Angelov, V.M. Garamus, M. Drechsler, *J. Mol. Liquids*, **2019**, *279*, 518-523. (c) L. van't Hag, X. Li, T.G. Meikle, S.V. Hoffmann, N.C. Jones, J.S.; Pedersen, A.M. Hawley, S.L. Gras, C.E. Conn, C.J. Drummond, *Langmuir*, **2016**, *32*, 6882–6894.

[19] (a) C. E. Conn, O. Ces, A. M. Squires, X. Mulet, S. M. Finet, R. H. Templer, J. M. Seddon, R. Winter, *Langmuir*, **2008**, *24*, 2331-2340. (b) A. Angelova, M. Drechsler, V.M. Garamus, B. Angelov, *ACS Omega* **2018**, *3*, 3235–3247. (c) C.Fong, T. Le, C.J. Drummond, *Chem. Soc. Rev.* **2012**, *41*, 1297–1322. (d) C.V. Kulkarni, A. Yaghmur, M. Steinhart, M.; Kriechbaum, M.; Rappolt, *Langmuir*, **2016**, *32*, 11907-11917.

[20] (a) C. Géral, A. Angelova, B. Angelov, V. Nicolas, S. Lesieur, Chapter 11, In "*Self-Assembled Supramolecular Architectures: Lyotropic Liquid Crystals*". N. Garti, P. Somasundaran, R. Mezzenga, Eds. (John Wiley & Sons, Inc., New Jersey), **2012**, pp. 319-355. (b) B. Angelov, A. Angelova, V. M. Garamus, M. Drechsler, R. Willumeit, R. Mutafchieva, P. Štěpánek, S. Lesieur, *Langmuir* **2012***, 28*, 16647-16655; (c) B. Angelov, A. Angelova, B. Papahadjopoulos-Sternberg, S.V. Hoffmann, V. Nicolas, S. Lesieur, *J. Phys. Chem. B,* **2012***, 116*, 7676-7686; (d) A. Angelova, C. Fajolles, C. Hocquelet, F. Djedaïni-Pilard, S. Lesieur, V. Bonnet, B. Perly, G. Le Bas, L. Mauclaire, J. Colloid Interface Sci. 2008, 322, 304-314; (e) A. Angelova, V.M. Garamus, B. Angelov, Z. Tian, Y Li, A. Zou, *Adv. Colloid Interface Sci.*, **2017**, *249*, 331-345.

[21] (a) C. Boyer, J.A. Zasadzinski, *ACS Nano* **2007***, 1*, 3, 176-182; (b) D. Danino, *Curr. Opin. Coll. Interface Sci.* **2012***, 17*, 316-329; (c) C. Schmitt, A.H. Lippert, N. Bonakdar, V. Sandoghdar, L.M. Voll, *Front Bioeng Biotechnol.* **2016***, 4*, 19; (d) H. v. Berlepsch, B. N. S. Thota, M. Wyszogrodzka, S. de Carlo, R. Haag, C. Böttcher, *Soft Matter,* **2018***, 14*, 5256-5269.

[22] (a) K. Chong, Y. Deng, *Methods Cell Biol.* **2012**, *108*, 317-43. (b) Y. Deng, Z.A. Almsherqi, *Interface Focus* **2015**, *5*, 20150012.

[23] (a) K. Veith, M. Martinez Molledo, Y. Almeida Hernandez, I. Josts, J. Nitsche, C. Löw, H. Tidow, *Chembiochem.* **2017**, *18*, 1735-1742; (b) X. Wang, G. Huang, D. Yu, B. Ge, J. Wang, F. Xu, F. Huang, H. Xu, J.R. Lu*, PLoS One.* **2013***, 8*, e76256; (c) Q. Zou, M. Abbas, L. Zhao, S. Li, G. Shen and X. Yan, *J. Am. Chem. Soc.,* **2017***, 139*, 1921-1927.

[24] (a) D.G Fatouros, D.A. Lamprou, A.J. Urquhart, S.N. Yannopoulos, I.S. Vizirianakis, S. Zhang, S. Koutsopoulos, *ACS Appl Mater Interfaces*. **2014**, *6*, 8184-9; (b) H. Cui, A.G. Cheetham, E.T. Pashuck, S.I. Stupp, *J. Am. Chem. Soc.,* **2014**, *136*, 12461-12468; (c) V. Castelletto, G. Cheng, C. Stain, C. J. Connon, I.W. Hamley, *Langmuir* **2012**, *28*, 11599–11608.

[25] (a) C.E. Blanchet, A. Spilotros, F. Schwemmer, M.A. Graewert, A. Kikhney, C.M. Jeffries, D. Franke, D. Mark, R. Zengerle, F. Cipriani, S. Fiedler, M. Roessle, D.I. Svergun, *J Appl Crystallogr.* **2015**, *48*(Pt 2) 431-443; (b) D.I. Svergun, M. H. J. Koch, P.A. Timmins, R.P. May, *Small Angle X-Ray and Neutron Scattering from Solutions of Biological Macromolecules*. Oxford University Press, Oxford, **2013**., pp. 286-319.

Entry for the Table of Contents

FULL PAPER

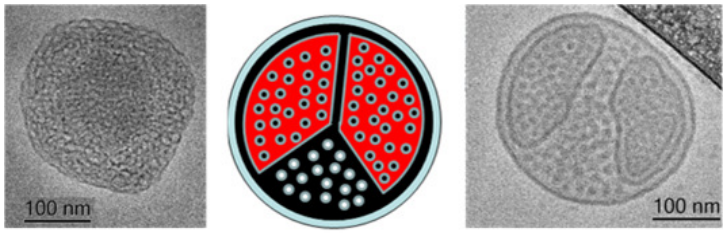

Multicompartment topologies of pep-lipid cubosomes and vesicles enclosing micelles, co-assembled with an unusual organizational complexity using multiple neuroprotective building blocks, and suitable as nanostructured membrane-mimetic environment for the sustained delivery of the class B GPCR ligand Pituitary Adenylate Cyclase-Activating Polypeptide (PACAP38) coupled to the lipid trophic factor docosahexaenoic acid (DHA).

Angelina Angelova, Markus Drechsler, Vasil M. Garamus, Borislav Angelov*

Page No. – Page No.

Pep-Lipid Cubosomes and Vesicles Compartmentalized by Micelles from Self-Assembly of Multiple Neuroprotective Building Blocks Including a Large Peptide Hormone PACAP-DHA

Additional Author information for the electronic version of the article.

Angelina Angelova: ORCID 0000-0002-0285-0637
Markus Drechsler: ORCID 0000-0001-7192-7821
Vasil M. Garamus: ORCID 0000-0001-9315-4188
Borislav Angelov: ORCID 0000-0003-3131-4822